Characterisation of coral explants: a model organism for cnidarian-dinoflagellate studies

Stephanie G. Gardner, Daniel A. Nielsen, Katherina Petrou, Anthony W. D. Larkum and Peter J. Ralph

Plant Functional Biology and Climate Change Cluster and the School of the Environment, University of Technology, Sydney, NSW, Australia

PO BOX 123 Broadway, NSW 2007, Australia

Communicating Author:

Katherina Petrou

Email: Katherina.Petrou@uts.edu.au

Tel: +61 2 9514 4159

Fax: +61 2 9514 4079

Keywords

Explant culture | Cnidarian-dinoflagellate symbiosis | *Symbiodinium* | Photophysiology | Respiration

Abstract

Coral cell cultures made from reef-building scleractinian corals have the potential to aid in the pursuit of understanding of the cnidarian-dinoflagellate symbiosis. Various methods have previously been described for the production of cell cultures *in vitro* with a range of success and longevity. In this study, viable tissue spheroids containing host tissue and symbionts (coral explants) were grown from the tissues of *Fungia granulosa*. The cultured explants remained viable for over two months and showed morphological similarities in tissue structure and internal microenvironment to reef-building scleractinian corals. The photophysiology of the explants (1 week old) closely matched that of the parent coral *F. granulosa*. This study provides the first empirical basis for supporting the use of coral explants as laboratory models for studying coral symbioses. In particular, it highlights how these small, self-sustaining, skeleton-free models can be useful for a number of molecular, genetic and physiological analyses necessary for investigating host-symbiont interactions at the microscale.

Introduction

Cnidarian-dinoflagellate symbioses are widespread in the marine environment, with the most well-known and arguably most ecologically important being that of scleractinian, reef-building corals (Furla et al. 2005; Rosic and Dove 2011). Historically, molecular, genetic and physiological analyses of cellular processes in corals have been difficult to conduct mainly because of the physiological complexities associated with differentiating processes and responses from the different organisms that make up the coral holobiont: namely the cnidarian animal, the photosynthetic dinoflagellate and other microbial partners (Reshef et al. 2006). In addition, many analyses are hindered by the presence of a calcium carbonate skeleton or the calcification process, which utilises the calicoblastic layer to deposit calcium carbonate (Davy et al. 2012). To get around these problems, many studies have made use of symbiotic dinoflagellates (belonging to the genus *Symbiodinium*) freshly isolated from the coral host to investigate the physiology of the symbiotic counterpart. While this method of investigation

50 helps to differentiate the dinoflagellate response from the animal, the act of isolating and/or culturing
51 *Symbiodinium in vitro* is unlikely to be directly representative of conditions *in hospite.* In symbiosis,
52 the intracellular environment regulated by the host cell has different chemical properties than that of
53 seawater (such as osmotic potential), and changing these conditions can induce stress responses in the
54 cultured cells that would otherwise not be present (Wang et al. 2011). Understanding of the coral
55 symbiosis would be greatly enhanced if it were possible to maintain cultures of symbiotic
56 zooxanthellae still encased in their host endoderm cells, but without the calicoblastic layer. However,
57 while such a culture would allow for detailed investigations of the symbiosis at the single cell level,
58 all attempts to isolate and maintain such cell lines have previously proven unsuccessful (Gates and
59 Muscatine 1992).
60
61 Recent work on coral tissue has led to new techniques for producing cultures of host tissue containing
62 viable symbionts that have been reported to survive between 52 h (Nesa and Hidaka 2009) and 1
63 month (Domart-Coulon et al. 2001) with one reporting survival of more than 3 years (Vizel et al.
64 2011). In particular, solitary fungiid corals have been key in developing and improving culturing of
65 coral tissues because they possess the ability to repair and regenerate their tissue and use budding as a
66 mode of survival when repair is impossible (Kramarsky-Winter and Loya 1996). In their study, tissue
67 fragments removed from budding *Fungia granulosa* were shown to develop into planula-like balls
68 that settled, attached and grew into new, fully differentiated individual corals.
69
70 Previous studies on coral explants have described various methods for producing a skeleton-free coral
71 and have shown coral explants to be good representatives or models of coral holobiont tissue (Nesa
72 and Hidaka 2009; Vizel et al. 2011), in that they contain ectoderm and endoderm cells separated by a
73 mesoglea (Tambutté et al. 2007). However, to date there has been no investigation into the actual
74 physiology of explants or their physiological response to environmental conditions, nor a comparison
75 of that response to whole parental corals.

In this study, using the solitary free-living coral *F. granulosa,* the internal microenvironment and tissue morphology of coral explants was characterised and the photophysiology of explants were compared with that of the parent coral *F. granulosa*. The aim of this study was to determine the suitability of these explants as model organisms for detailed studies into coral symbioses and validate their usefulness for studying tissue functions and processes such as those involved in cnidarian-dinoflagellate symbiosis, cell interactions, proliferation, growth and differentiation and disease, without the skeleton.

Materials and Methods

Coral Collection

Individual solitary corals of the species *F. granulosa* were collected from the lagoon at Heron Island, Great Barrier Reef, Australia (151° 55′ E, 23° 26′ S) and maintained in shaded aquaria (< 100 μmol photons m^{-2} s^{-1}) at ambient lagoon temperature (25 °C) for 1 week before being transported to the University of Technology, Sydney, where they were maintained at 25 ± 0.5 °C, at a salinity of 34 ppt and pH 8.2. Corals were maintained at 200 μmol photons m^{-2} s^{-1} of light, provided by metal halide lamps (400 W, Ablite with 40 W Power-Glo fluorescent bulb) in a 12:12 h light:dark cycle.

Explant production and viability

Explants were produced following the method described in Vizel et al. (2011) with a few modifications. Briefly, coral fragments were removed by cutting a small wedge of skeleton and tissue (approximately 1.5 cm in width and 2 cm in length) from the parental coral with a pair of bone cutters. Each sample was left to stand for 2 h in filtered seawater (FSW, 0.22 μm) containing antibiotics (Gentamicin and Kanamycin, both 50 μg ml^{-1}, Life Technologies Australia Pty Ltd, Mulgrave, Victoria) in order to minimise bacterial contamination. Coral tissue, consisting of both ectoderm and endoderm, was gently peeled from the skeleton using fine forceps and placed into autoclaved

borosilicate glass dishes (Schott-DURAN®, GmbH, Germany) containing 50 ml FSW and antibiotics (see above). Tissue fragments were broken into smaller pieces and skeleton fragments were carefully removed with a sterile transfer pipette. After 24 h, explants ranging between 400 – 800 μm in diameter began to form. Any viable explants (characterised as negatively buoyant round motile balls containing both *Symbiodinium* and host tissues encased in a mucus layer) were then transferred to new sterile glass petri-dishes containing FSW and antibiotics, and maintained at a density of up to 30 explants per dish. The antibiotic treatment was applied for the first two days, after which explants were maintained in antibiotic-free FSW to allow explants to re-establish their microbiota. At this stage, a small piece of pink encrusting coralline algae (*Lithothamnion* sp.) was added to each dish to provide cues to the growing explants, as it is known to induce coral metamorphosis (Heyward and Negri 1999). Every three days, explants were transferred into clean petri dishes with fresh FSW and coralline algae. This modified culturing method was used because preliminary trials did not yield viable explants in the absence of antibiotics, due to strong bacterial growth. Tests for long-term negative effects of the antibiotics on the explant symbiont health using PAM fluorometry were also conducted and the data showed no measurable effect of the long-term antibiotic treatment compared with those washed after only 2 days of exposure (data not shown). However, to minimise any potential undetectable effects, treatment with antibiotics was limited to only the first two days, until explant formation. Cultured explants were maintained under 100 μmol photons m^{-2} s^{-1} of light (Aquablue Plus T5 HO fluorescent light system; Giesemann Aquaristic GmbH, Nettetal, Germany) on a 10:14 h light:dark regime. Light intensity was measured with a light meter (Li-250A, Li-Cor, Lincoln, Nebraska, USA) and the temperature of the culture was maintained at 25 ± 0.5 °C using a 25W aquarium heater (Aqua One, Ingleburn, NSW). Explant viability was monitored for 63 days using chlorophyll *a* fluorescence (see method below).

Morphology

Explant morphology through optical sectioning was visualised using an upright epifluorescence microscope (Olympus BX51) equipped with a DP70 CCD colour camera. Fluorescence was detected using various filter sets: red for *Symbiodinium* chlorophyll autofluorescence (excitation 688 nm/ emission 679-754 nm), narrow green (excitation 470 nm/ emission 510-550 nm) and wide blue (excitation 330-385 nm/ emission 420 nm) for host fluorescent pigment proteins. Images were captured using the DP Controller software (version 1.2.1.108; Olympus Optical Co. Ltd). Individual symbiont and animal endoderm cell viability was assessed using the viability stain Glycine, N,N'-[[3',6'-bis(acetyloxy)-3-oxospiro[isobenzofuran-1(3H),9'-[9H]xanthene]-4',5'-diyl]bis(methylene)]bis[N-[2-[(acetyloxy)methyoxy]-2-oxoethyl]-, bis[(acetyloxy)methyl] ester/ N/A (referred to as Calcein-AM; 8 µM final concentration) and nucleic acid stain 2,5'-Bi-1H-benzimidazole, 2'-(4-ethoxyphenyl)-5-(4-methyl-1-piperazinyl)-/ 23491-52-3 (referred to as Hoechst; 4 µM final concentration; both Life Technologies, Australia Pty Ltd). Explants were incubated in these stains for 40 min, and then washed in FSW before being flattened onto a slide using a cover slip to break apart the internal structure. Individual cells were imaged (400x final magnification) on an inverted fluorescence microscope (Nikon Eclipse T*i*, Nikon Instruments Inc., Melville, NY, USA) using the standard filters TxRed (red fluorescence), FITC (green fluorescence) and DAPI (blue fluorescence) for chlorophyll autofluorescence, Calcein-AM and Hoechst, respectively.

Chlorophyll *a* fluorescence

Explant viability was estimated by measuring symbiont chlorophyll *a* fluorescence every three days over a two-month period. Variable fluorescence was measured using a Pulse Amplitude Modulated (PAM) fluorometer (Imaging PAM –Max/K, RGB, Walz GmbH, Effeltrich, Germany), mounted on a compound microscope (Axiostar plus, Zeiss, Germany). Explants were placed onto a microscope well-slide and dark-adapted for 10 min prior to measurements. Measurements were taken (200x final magnification) using Imaging Win software (V2.32 FW Multi RGB; Walz GmbH, Effeltrich,

Germany). Following 10 min dark-adaptation, minimum fluorescence (F_O) was recorded before application of a high intensity saturating pulse of light (saturating pulse width = 0.8 s; saturating pulse intensity > 3000 µmol photons m^{-2} s^{-1}), where maximum fluorescence (F_M) was determined. From these two parameters the maximum quantum yield of PSII was calculated as $F_V/F_M = (F_M-F_O)/F_M$ (Schreiber 2004). For more detailed photophysiological investigation, steady-state light curves (SSLC) were conducted on 1-week old explants. Explants were placed onto a microscope well-slide in a solution of 7% $MgCl_2$ (to reduce movement - see below), and dark-adapted for 10 min prior to measurements. Seven actinic light levels (5, 20, 29, 84, 157, 203, 313 µmol photons m^{-2} s^{-1}) were applied for 3 min each before recording the light-adapted minimum (F_T) and maximum fluorescence (F_M') values. For comparison between explant physiology and that of a coral, a nine-step SSLC was also conducted on *F. granulosa* using the Imaging PAM (Max/K, Walz GmbH, Effeltrich, Germany) at similar actinic light levels (11, 21, 36, 81, 111, 231, 336, 461, 701 µmol photons m^{-2} s^{-1}) for 3 min. From the SSLCs, photophysiological parameters, dark-adapted maximum quantum yield of PSII (F_V/F_M), light-adapted effective quantum yield (Φ_{PSII}), non-photochemical quenching (NPQ) and relative electron transport rate (rETR) were obtained (see Schreiber 2004 for details). The rETR from the SSLCs were fitted to a double exponential function and all photosynthetic parameters from the curve fit; light utilisation efficiency (α), minimum saturating irradiances (E_K), and maximum relative electron transport rate ($rETR_{MAX}$), were obtained as described in Ralph & Gademann (2005). Following all chlorophyll *a* fluorescence measurements, explants were transferred back into FSW and left for 30 min in darkness before F_V/F_M was re-measured in order to assess any negative effect of the $MgCl_2$ treatment.

To prevent ciliary-activated rotation of the explants during microscopy measurements, a 7% magnesium chloride ($MgCl_2$) solution in FSW (0.22 µm) was used. Magnesium chloride is a commonly used method for anaesthetising animal cells (Messenger et al. 1985), because it only inhibits movement while allowing cellular processes to continue. In a preliminary experiment using the Imaging PAM, no significant difference in effective quantum yield of PSII (Φ_{PSII}) was detected

between the explants anaesthetised in $MgCl_2$ and non-anaesthetised explants ($F_{1, 10} = 0.681$, $p = 0.428$, $n = 6$), and explants regained ciliary activity within 5 mins of being transferred back into FSW.

Microprofiling

Oxygen and pH microprofiling was used to characterise the internal chemical and metabolic regions of 1-week old explants. Explants were positioned on a layer of solidified, saline agar (0.75%, 35 ppt) in a petri-dish and a single droplet of dissolved agar (Agar for microbiology, Fluka Analytical, Sigma-Aldrich, USA), pre-cooled in a water bath to just above gelation temperature (35 °C), was placed on top of each explant to encase them. The drop of agar cooled and solidified almost immediately, minimising potential temperature shock. While the agar fixed the explant in place, it did not prevent the explant from spinning around its own axis inside the agar, indicating that the explant was still alive and active. The petri dish with the fixed explant was then positioned in a temperature controlled (25 ± 0.5 °C) flow chamber (flow rate approx. 2 cm s^{-1}) and left to acclimate for at least 20 min before profiling. Light was supplied (at close to growth irradiance, approximately 90 µmol photons m^{-2} s^{-1}) via a fibre optic tungsten-halogen light source (KL-2500, Schott, Germany) equipped with a collimating lens.

Oxygen and pH profiles were measured on individual explants with a Clark type oxygen microsensor (Ø = 25 µm, 90% response time < 2 s, stirring sensitivity < 1%) and a pH microsensor (Ø = 50 µm, 90% response time < 10 s) (both Unisense A/S, Denmark) with an external standard 2 mm reference electrode (Ionode LLC, Australia). Both sensors were connected to a multimeter (Unisense A/S, Denmark), which in turn was connected to a laptop computer onto which the acquired signal was logged using dedicated software (SensorTrace Pro v.3.1.1, Unisense A/S, Denmark). The oxygen microsensor was calibrated according to the manufacturer protocol immediately prior to measurements using a freshly prepared sodium thiosulfate solution (10% w/w) and air-bubbled FSW at experimental temperature (25 °C) as 0% and 100% air saturation values, respectively. The pH

electrode was calibrated via a linear fit to the millivolt output measured in pH 4, 7 and 10 buffers, resulting in a slope of ~54 mv pH^{-1}.

The microsensors were positioned and moved via a micro-profiler stepper motor (Unisense A/S, Denmark) controlled by software (SensorTrace Pro). Before each profile, the microsensor was positioned at the surface of the explant (defined as 0 mm depth) viewed through a stereo-microscope supported by an articulating arm. Each profile was started at a distance above the surface of the explant (0.5 - 1.0 mm) and all profiles were carried out in steps of 25 and 100 μm for oxygen and pH, respectively. For dark profiles, the microsensor was positioned at the explant surface under low light, after which the light was turned off and the explant was left to dark acclimate for 15 min prior to profiling. Due to the inherent fragility of the explants, profiling was kept to a minimum in order to ensure maximum structural integrity over the series of light/dark O_2 and pH measurements. As a result, no replicate measurements were carried out on the same individual explant. To determine the net photosynthetic response time of the explants, oxygen concentrations were measured during a series of light/dark cycles. Using the same flow chamber set up as the microprofiles, the oxygen sensor was positioned with a manual micromanipulator at the centre of the explant, while the light was switched on and off in 5 min intervals and oxygen concentration logged every 2 s using the data acquisition software (SensorTrace Basic, Unisense A/S, Denmark). All microsensor measurements were conducted on individual explants for all profiles (n = 3).

Results

Explant viability and morphology

Explants ranged in diameter between 430-800 μm with an average volume of $1.7\times10^6 \pm 7.3\times10^7$ μm^3 (mean ± SD; n = 12). They were viable for over two months, where the effective quantum yield of PSII (Φ_{PSII}) remained constant for 63 days (0.517 ± 0.007; n = 32). While measurements were not

continued beyond 63 days, explants remained viable for an additional 2 months (personal observation).

The multiple layers of host tissue present in whole explants were investigated via light microscopy (Fig. 1). The images clearly show the internal complexity of these organisms and highlight the similarity in tissue structure to reef-building corals (Fig. 1a-c). Light microscopy revealed a thin surface ectoderm (Ec) coated with a mucus layer (Ml) and external cilia (not visible in these images) forming the outer part of the explant (Fig. 1a). Also visible is an intermediate mesogleal (Me) tissue layer bordering the inner edge of the ectodermal membrane (Fig. 1b). Similar structures can be seen in an optical section of the parental *F. granulosa* coral (Fig. 1c), with an outer ectoderm and zooxanthellae housed in endodermal tissue. Closer inspection of the endodermal tissue and inner cavity of the explants shows individual symbiotic zooxanthellae (Zs) surrounded by host cnidarian endodermal (En) cell membranes with host nuclei (N) (Fig. 1d). In addition, some zooxanthellae, not encased in a host animal cell (Z), were also identified (Fig. 1d). Epifluorescence microscopy showed the explants to contain a suite of blue, green and yellow fluorescent pigment proteins in the host tissue, as well as the red autofluorescence from the chlorophyll in the plastids of the zooxanthellae (Fig. 1e, f).

Steady-state light curves

Steady state light curves (SSLC) that were performed on the explant show a decline in effective quantum yield of PSII (Φ_{PSII}) from 0.6 at the lowest irradiance (5 µmol photons m^{-2} s^{-1}) to 0.15 at the highest irradiance (313 µmol photons m^{-2} s^{-1}; Fig. 2a). This was countered by a concomitant rise in non-photochemical quenching (NPQ) with increasing irradiance, reaching a maximum of approx. 1.5 a.u at maximum irradiance (Fig. 2a). A comparable response was measured in the parent coral *F. granulosa*, where Φ_{PSII} declined from 0.6 to 0.16 and an increase in NPQ 1.5 a.u at maximum irradiance (700 µmol photons m^{-2} s^{-1}; Fig. 2b). Comparison of relative electron transport rate (rETR)

257 measured in the explants and corals showed a difference in magnitude of around 50% (Fig. 2c, d) with
258 the $rETR_{MAX}$ for the explant (46.96 ± 8.19 a.u) being half of that measured in *F. granulosa* (105.55 ±
259 6.82 a.u; Table 1). Minimum saturating irradiance (E_K) for the explant was 58.91 ± 11.2 µmol photons
260 m^{-2} s^{-1} compared with 177 ± 6.9 µmol photons m^{-2} s^{-1} in the *F. granulosa* (Table 1). Light utilisation
261 efficiency (α), was higher for the explant (0.8 ± 0.02 a.u) compared with the coral (0.59 ± 0.02 a.u).
262 Independent-samples t-test comparing F_V/F_M for the explants and whole coral showed no significant
263 difference.
264

265 **O_2 and pH profiles**

266 Oxygen profiles showed that in two out of the three explants measured, the tissue became hyperoxic
267 in the light (up to 280 ± 84 µmol l^{-1}), as a result of symbiont photosynthesis, and hypooxic in the dark
268 (down to 112 ± 19 µmol l^{-1}) due to combined animal and symbiont respiration (Fig. 3a, b). In the case
269 of the third explant, no net evolution of O_2 was observed during the light and dark cycles, (Fig. 3c);
270 however, in all cases, the O_2 concentration was higher in the light than in the dark. The pH of the
271 explants followed a similar pattern; decreasing in the dark by an average of 0.5 pH units from the
272 outer edge of the explant (pH 8.23 ± 0.04) to an internal pH 7.77 ± 0.09 and increasing in the light by
273 up to 0.6 pH units from the outer edge to an average of pH 8.55 ± 0.41 inside the explant (Fig. 3). As
274 expected, the explant with no net O_2 evolution showed no increase above ambient pH in the light (Fig.
275 3c).
276

277 The explants showed a rapid response to changes in light conditions; reaching maximum and
278 minimum internal oxygen equilibria concentrations in less than 5 min after onset of illumination or
279 darkness, respectively (Fig. 4). Steady state oxygen production was reached within the first few
280 minutes of irradiance (90 µmol photons m^{-2} s^{-1}), providing further confirmation for the 3 min used to
281 obtain steady state fluorescence in the explants. While dark equilibrium oxygen concentrations did
282 not vary much between individual explants, stabilising between 96 and 122 µmol l^{-1}, the equilibrium

concentration in the light varied considerably, stabilising at 134, 219 and 368 μmol l^{-1} in individual explants 1, 2 and 3, respectively (Fig. 4). This variability can most likely be explained by the differences in symbiont densities (data not shown). Only one of the three explants reached hyper-oxic conditions in the light (Fig. 4, black symbols), but all showed a net increase in oxygen concentration in the light.

Discussion

Explant production has been described previously (Kopecky and Ostrander 1999; Domart-Coulon et al. 2001; Domart-Coulon et al. 2004; Nesa and Hidaka 2008; Vizel et al. 2011; Lecointe et al. 2013), where viability has varied considerably, from 52 h (Nesa and Hidaka 2009), to more than 3 years (Vizel et al. 2011). The explants cultured here, using a modified version of the method described by Vizel et al. (2011), remained viable for more than 2 months with no apparent indications of reduced viability, suggesting that the explants were stable and able to survive significantly longer.

The average size of 'healthy' explants (defined in this study as having an effective quantum yield of PSII > 0.5 measured at growth irradiance) closely match those from earlier studies (Nesa and Hidaka 2009; Lecointe et al. 2013), with the exception of a few larger explants (up to 1500 μm), which were generally seen to have a lower survival rate (< 14 days, personal observation). The larger explants often possessed an internal, fluid-filled cavity lined with cilia, a feature also described by Lecointe et al. (2013). This morphological development minimises tissue thickness and thus increases O_2 availability through the tissue, potentially allowing the explant to grow larger than would otherwise be possible. The observed lower viability of the larger explants may be the result of a reduced symbiont to host tissue ratio, at least in cases where symbiont density is low. This would result in increased metabolic demands on the larger explants due to a relatively low amount of carbon that is being generated by symbiont photosynthesis (Manzello and Lirman 2003; Starzak et al. 2014).

309 Interestingly, Nesa and Hidaka (2009) found no correlation between survival and explant size,
310 however, the overall viability of their explants was less than three weeks, suggesting they may not
311 have been stable or environmental conditions were not favourable for long-term survival.

312

313 Microscopy revealed coral explants possess similar arrangement and tissue components as found in
314 scleractinian corals (Kopecky and Ostrander 1999; Domart-Coulon et al. 2001; Kramarsky-Winter et
315 al. 2008) with the exception of the calicoblastic layer (Fig. 1a-c). Explants in this study had an outer
316 ectoderm covered in cilia and mucus, an endodermal cavity containing intracellular symbionts
317 (zooxanthellae) and a mesogleal layer separating the two tissues (Fig. 1a, b), similar to the parental *F.*
318 *granulosa* (Fig. 1c). Finer detail showed that the symbiotic zooxanthellae (Zs) were encased in host
319 endodermal tissue (En), a feature common with whole corals (Gates et al. 1992). This comparable cell
320 type composition provides a better means for investigating how nutrients and carbon are transferred
321 between the host and symbiont at a microscale (Davy and Cook 2001; Furla et al. 2005). Green
322 fluorescent pigments (GFP) were observed throughout the endodermal tissue (Fig. 1f) and were
323 heterogeneous in their spatial distribution. This heterogeneity indicates random organisation of the
324 tissues, in contrast to some adult corals, where a concentrated ring of GFP like molecules can often be
325 seen around the oral disk of the polyp (Lecointe et al. 2013). The function of fluorescent pigments in
326 corals have been attributed to two contradictory processes involving light-regulation; 1) they provide
327 photoprotection under high-light conditions, through the dissipation of excess energy at wavelengths
328 of low photosynthetic activity (Salih et al. 2000; Dove et al. 2008), and 2) they can enhance light
329 availability and hence photosynthesis under low-light conditions (Kawaguti 1969; Salih et al. 2000).
330 In some instances they are proposed to do both, depending on the position of the fluorescent pigment
331 relative to the zooxanthellae (Dove et al. 2001). In present study, it is possible that they fulfil a dual
332 role, as the explants were grown at relatively low light, and showed relative sensitivity to very high
333 light (Fig. 2).

334

335 The lack of difference between the maximum quantum yield of PSII (F_V/F_M) of the explants and the
336 whole parent coral provides evidence for no or limited change in the photosynthetic efficiency and
337 health of the coral tissue from its natural coral morphology to its new explant morphology (Table 1).
338 In general, the PAM data showed similar patterns in both the explants and the whole coral, typical of
339 high- and low-light acclimated photosystems (Fig. 2). The capacity of corals to acclimate to changes
340 in growth irradiance, such as those likely to occur following physical disturbances on reefs or from
341 competition for space, have been shown in studies comparing sun and shade-adapted corals,
342 harbouring the same *Symbiodinium* clades (Anthony and Hoegh-Guldberg 2003; Ulstrup et al. 2006).
343 In this study, all photophysiological parameters measured in the SSLCs for the explants were
344 approximately half of those determined in the whole parental coral, where, at the same light level, the
345 Φ_{PSII} of the explants was roughly half that measured in *F. granulosa* and the NPQ was the same for
346 explants at 310 µmol photons m^{-2} s^{-1} as it was for the parental corals at double that irradiance (700
347 µmol photons m^{-2} s^{-1}). These differences can be attributed to the differences in growth irradiance
348 (Ralph and Gademann 2005), where explants were grown at 50% of the light level of the parental
349 corals (Fig. 2). The $rETR_{MAX}$, E_K and increased α in the explant compared with the coral are typical
350 differences with respect to shade versus high-light acclimated phototrophs (Anthony and Hoegh-
351 Guldberg 2003), and provides further support for the influence of growth irradiance on the differences
352 in photophysiological response. Shade-adapted corals tend to have a higher α and a lower E_K
353 compared with high light adapted corals (Anthony and Hoegh-Guldberg 2003), which can be seen in
354 the explants with a lower growth irradiance compared with the corals. The fact that $rETR_{MAX}$ was
355 almost exactly 50% of that measured in the parental coral, also fits with work by Ralph and
356 Gademann (2005), who found the differences between the $rETR_{MAX}$ values of shade and high-light
357 acclimated seagrass matched the differences in their respective growth irradiance (in their case a 6
358 fold difference).

359

360 Microprofiling revealed an expected increase in photosynthetic activity with increasing explant
361 colouration (symbiont density) (Fig. 3), resulting in higher internal concentration of O_2 as well as

362 increased pH in the light, and conversely higher respiration rate (lower O_2 concentration) and lower
363 pH in the dark. The higher pH in the light than in the dark (Fig. 3), suggests an increase in carbon
364 dioxide uptake during photosynthesis. These results are similar to those found in previous studies on
365 the microenvironment of scleractinian corals, where photosynthesis in the light resulted in a build-up
366 of O_2 in the tissue and a pH of up to 8.6, whereas in the dark, O_2 concentration was reduced to < 2%
367 air saturation and pH dropped to between 7.3 and 7.4 (Kühl et al. 1995). In two of three explants,
368 profiling revealed O_2 accumulation in the light (130-170% saturation), indicating that those particular
369 explants were net autotrophic (Fig. 3a, b). While the respiration rate of corals vary between species
370 and depth (Stambler et al. 2008), most previous studies suggests that, in shallow waters, the coral-
371 algal association is largely autotrophic, with photosynthetic production by the algae well exceeding
372 respiration of algae and coral (Coles and Jokiel 1977). It is therefore likely that viable explants will
373 generally be net autotrophic, as a result of a favourable ratio between animal tissue and symbiont
374 density and activity.
375
376 The fast (< 5 min) equilibration between oxygen production and consumption in the explants (Fig. 4)
377 is comparable to oxygen responses that have been measured in corals (Kühl et al. 1995). However, in
378 contrast to the findings of Kühl et al. (1995), none of the explants investigated in this study became
379 anoxic in the dark. This is likely due to their small size, and a large surface area to volume ratio, thus
380 allowing for a sufficient supply of O_2 to be exchanged from the water-column.
381
382 Investigating stress responses at the cellular or tissue level are essential to better understand the
383 cnidarian-dinoflagellate symbiosis (Nesa and Hidaka 2009). This study has shown that coral explants,
384 produced from pieces of tissue, are photosynthetically viable and morphologically similar to coral
385 tissue at the micro scale, and therefore may constitute a model system with which to further our
386 understanding of cnidarian-dinoflagellate interactions. The small size of the explants allows for easy
387 manipulation under different environmental conditions, and the lack of a skeleton makes them ideal
388 for live imaging as whole organisms or investigating responses at the individual cell level. In addition,
389 these traits (comparable tissue structure and skeleton-free) make them potentially good model

organisms for studying the optical properties of coral tissue. This method of culturing coral tissue opens up the possibility for studying coral physiology, symbiosis and development of corals and it allows for the use of modern microscale techniques to investigate the effects of environmental stresses on these fundamental biological concepts.

Acknowledgements

We would like to thank the two anonymous reviewers for their helpful comments and suggestion for improvements on the manuscript. We would like to also extend thanks to Cheryl Woodley, Sylvia Galloway, Athena Burnett, Lisa May and Esti Winter (NOAA Charlestown, USA) for their advice on explant culture methodology. We are grateful for the technical assistance of Michael Johnson and Catherine Gorrie from the University of Technology, Sydney. Corals were collected under the Great Barrier Reef Marine Park Authority permits G11/34670.1 and G09/31733.1 issued to PJR. SG was supported by an Australian Postgraduate Award (APA), and research funding was provided by the Plant Functional Biology and Climate Change Cluster (C3) and the School of the Environment, University of Technology, Sydney.

References

Anthony KRN, Hoegh-Guldberg O (2003) Variation in coral photosynthesis, respiration and growth characteristics in contrasting light microhabitats: An analogue to plants in forest gaps and understoreys? Funct Ecol 17:246–259

Coles SL, Jokiel PL (1977) Effects of temperature on photosynthesis and respiration in hermatypic corals. Mar Biol 43:209-216

Davy SK, Cook CB (2001) The relationship between nutritional status and carbon flux in the zooxanthellate sea anemone *Aiptasia pallida*. Mar Biol 139:999-1005

Davy SK, Allemand D, Weis VM (2012) Cell biology of cnidarian-dinoflagellate symbiosis. Microbiol Mol Biol Rev 76:229-261

Domart-Coulon I, Tambutté S, Tambutté E, Allemand D (2004) Short term viability of soft tissue detached from the skeleton of reef-building corals. J Exp Mar Biol Ecol 309:199– 217

Domart-Coulon I, Elbert DC, Scully EP, Calimlim PS, Ostrander GK (2001) Aragonite crystallization in primary cell cultures of multicellular isolates from a hard coral, *Pocillopora damicornis*. Proc Natl Acad Sci USA 98:11885–11890

Dove SG, Hoegh-Guldberg O, Ranganathan S (2001) Major colour patterns of reef building corals are due to a family of GFP-like proteins. Coral Reefs 19:197-204

Dove SG, Lovell C, Fine M, Deckenback J, Hoegh-Guldberg O, Iglesias-Prieto R, Anthony KRN (2008) Host pigments: Potential facilitators of photosynthesis in coral symbioses. Plant Cell Environ 31:1523-1533

Furla P, Allemand D, Shick JM, Ferrier-Pagès C, Richier S, Plantivaux A, Merle PL, Tambutté S (2005) The Symbiotic Anthozoan: A physiological chimera between alga and animal. Integrative and Comparative Biology 45:595-604

Gates RD, Muscatine L (1992) Three methods for isolating viable anthozoan endoderm cells with their intracellular symbiotic dinoflagellates. Coral Reefs 11:143-145

Gates RD, Baghdasarian G, Muscatine L (1992) Temperatures causes host cell detachment in symbiotic cnidarians: Implications for coral bleaching. The Biological Bulletin 182:324-332

Heyward AJ, Negri AP (1999) Natural inducers for coral larval metamorphosis. Coral Reefs 18:273-279

Kawaguti S (1969) Effect of the green fluoresent pigment on the productivity of reef corals. Micronesica 5:313

Kopecky EJ, Ostrander GK (1999) Isolation and primary culture of viable multicellular endothelial isolates from hard corals. In Vitro Cell Dev Biol Anim 35:616-624

Kramarsky-Winter E, Loya Y (1996) Regeneration versus budding in fungiid corals: A trade-off. Mar Ecol Prog Ser 134:179-185

Kramarsky-Winter E, Loya Y, Vizel M, Down CA (2008) Method for coral tissue cultivation and propagation. Ramot at Tel Aviv University (ed)

Kühl M, Cohen Y, Dalsgaard T, Jergensen BB, Revsbech NP (1995) Microenvironment and photosynthesis of zooxanthellae in scleractinian corals studied with microsensors for O_2, pH and light. Mar Ecol Prog Ser 117:159-172

Lecointe A, Cohen S, Gèze M, Djediat C, Meibom A, Domart-Coulon I (2013) Scleractinian coral cell proliferation is reduced in primary culture of suspended multicellular aggregates compared to polyps. Cytotechnology 65:705-724

Manzello D, Lirman D (2003) The photosynthetic resilience of *Porites furcata* to salinity disturbance. Coral Reefs 22:537–540

Messenger JB, Nixon M, Ryan KP (1985) Magnesium chloride as an anesthetic in cephalopods. Comp Biochem Physiol C 82:203-205

Nesa B, Hidaka M (2008) Thermal stress increases oxidative DNA damage in coral cell aggregates. Proc 11th Int Coral Reef Symp, 7-11 July

Nesa B, Hidaka M (2009) High zooxanthella density shortens the survival time of coral cell aggregates under thermal stress. J Exp Mar Biol and Ecol 368:81-87

Ralph PJ, Gademann R (2005) Rapid light curves: A powerful tool to assess photosynthetic activity. Aquat Bot 82:222-237

Reshef L, Koren O, Loya Y, Zilber-Rosenberg I, Rosenberg E (2006) The coral probiotic hypothesis. Environ Microbiol 8:2068-2073

Rosic NN, Dove S (2011) Mycosporine-Like Amino Acids from Coral Dinoflagellates. Appl Environ Microbiol 77:8478–8486

Salih A, Larkum AWD, Cox G, Kühl M, Hoegh-Guldberg O (2000) Fluorescent pigments in corals are photoprotective. Nature 408:850-853

Schreiber U (2004) Pulse-amplitude-modulation (PAM) fluorometry and saturation pulse method: an overview. In: Papageorgiou GC, Govindjee (eds) Chlorophyll *a* fluorescence. Springer Netherlands, pp 279-319

Stambler N, Levy O, Vaki L (2008) Photosynthesis and respiration of hermatypic zooxanthellate Red Sea corals from 5-75m depth. Isr J Plant Sci 56:45-53

Starzak DE, Quinnell RG, Nitschke MR, Davy SK (2014) The influence of symbiont type on photosynthetic carbon flux in a model cnidarian–dinoflagellate symbiosis. Mar Biol 161:711-724

Tambutté E, Allemand D, Zoccola D, Meibom A, Lotto S, Caminiti N, Tambutté S (2007) Observations of the tissue-skeleton interface in the scleractinian coral *Stylophora pistillata*. Coral Reefs 26:517-529

Ulstrup KE, Ralph PJ, Larkum AWD, Kuhl M (2006) Intra-colonial variability in light acclimation of zooxanthellae in coral tissues of *Pocillopora damicornis*. Mar Biol 146:1325–1335

Vizel M, Loya Y, Downs CA, Kramarsky-Winter E (2011) A novel method for coral explant culture and micropropagation. Mar Biotechnol 13:423-432

Wang JT, Meng PJ, Sampayo E, Tang SL, Chen CA (2011) Photosystem II breakdown induced by reactive oxygen species in freshly-isolated *Symbiodinium* from *Montipora* (Scleractinia; Acroporidae). Mar Ecol Prog Ser 422:51-62

Figure Legends

Fig 1 Explant structure (1 week old) showing; a & b) differential interference contrast (DIC) of zooxanthellae (Z), the ectoderm (Ec), mucus layer (Ml), endoderm (En) and mesoglea (Me) at two different focal planes (200x, scale bar 50 µm), c) structure of an optical section from *Fungia granulosa* including; zooxanthellae (Z), the ectoderm (Ec) and endoderm (En) (200x, scale bar 50 µm), d) endosymbiotic zooxanthellae (Zs) cells (red) in a coral explant, surrounded by Calcein-AM stained cnidarian endoderm (En) cells (green) with Hoechst-stained nuclei (N) (blue) and zooxanthellae (Z) not encased in a host animal cell (400x, scale bar 10 µm), and explant autofluorescence using e) wide blue and f) narrow green filters on the epifluorescence microscope (200x, scale bar 50 µm).

Fig 2 Effective quantum yield of photosystem II ($\Phi_{PSII;}$ grey triangles), and non-photochemical quenching (NPQ; black circles) as a function of irradiance for a) the explants grown at 100 µmol photons m^{-2} s^{-1} (1 week old), b) *Fungia granulosa* grown at 200 µmol photons m^{-2} s^{-1}. Relative electron transport rate (rETR) as a function of irradiance for c) explants and d) *F. granulosa*. Fluorescence images of e) a dark-adapted explant at 200x magnification taken on the Microscopy Imaging PAM and f) dark-adapted *F. granulosa* taken at the beginning of the light curve on the Maxi Head Imaging PAM. Data represent the mean ± SE (n = 3-4). Scale bar on e) is 100 µm and f) is 2cm.

Fig 3 Oxygen concentration (circle symbols; top x-axis) and pH (triangle symbols; bottom x-axis) profiles of individual explants (1 week old) in the light (white symbols) and dark (black symbols). The solid black line indicates the top of the explant (defined as 0 mm depth) and the dotted line shows the position of the bottom of the explant.

Fig 4 The oxygen concentration of three individual explants (1 week old) measured in 5 min light:dark cycles using an oxygen microelectrode. The bars along the horizontal axis indicate the

periods of darkness (black) and 90 µmol photons m^{-2} s^{-1} (white). The respective diameters of the explants measured were 1 = 648 µm, 2 = 852 µm and 3 = 1010 µm. The dotted line indicates the oxygen saturation point in seawater (220 µmol l^{-1}) under experimental conditions.

Figures:

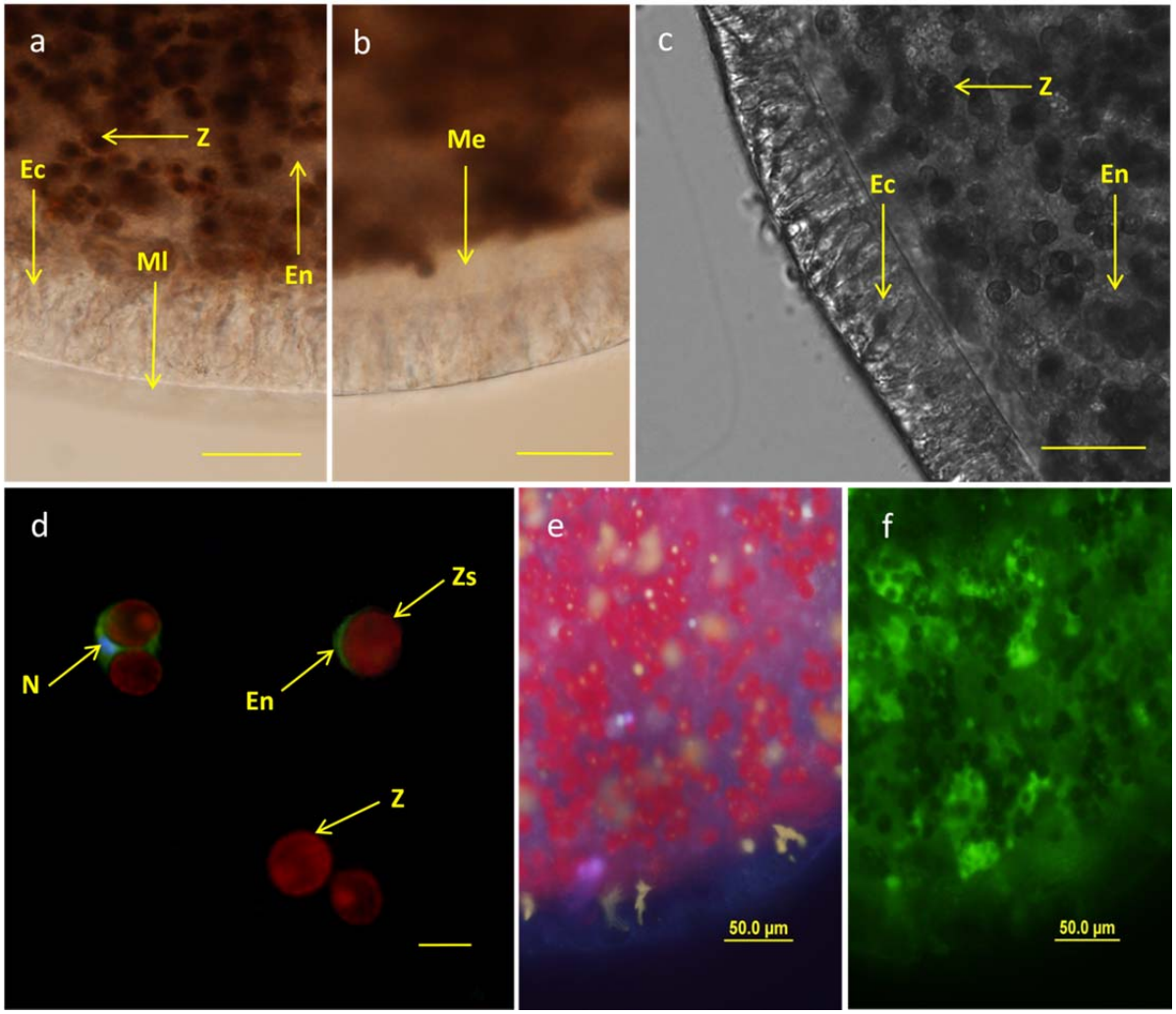

Figure 1

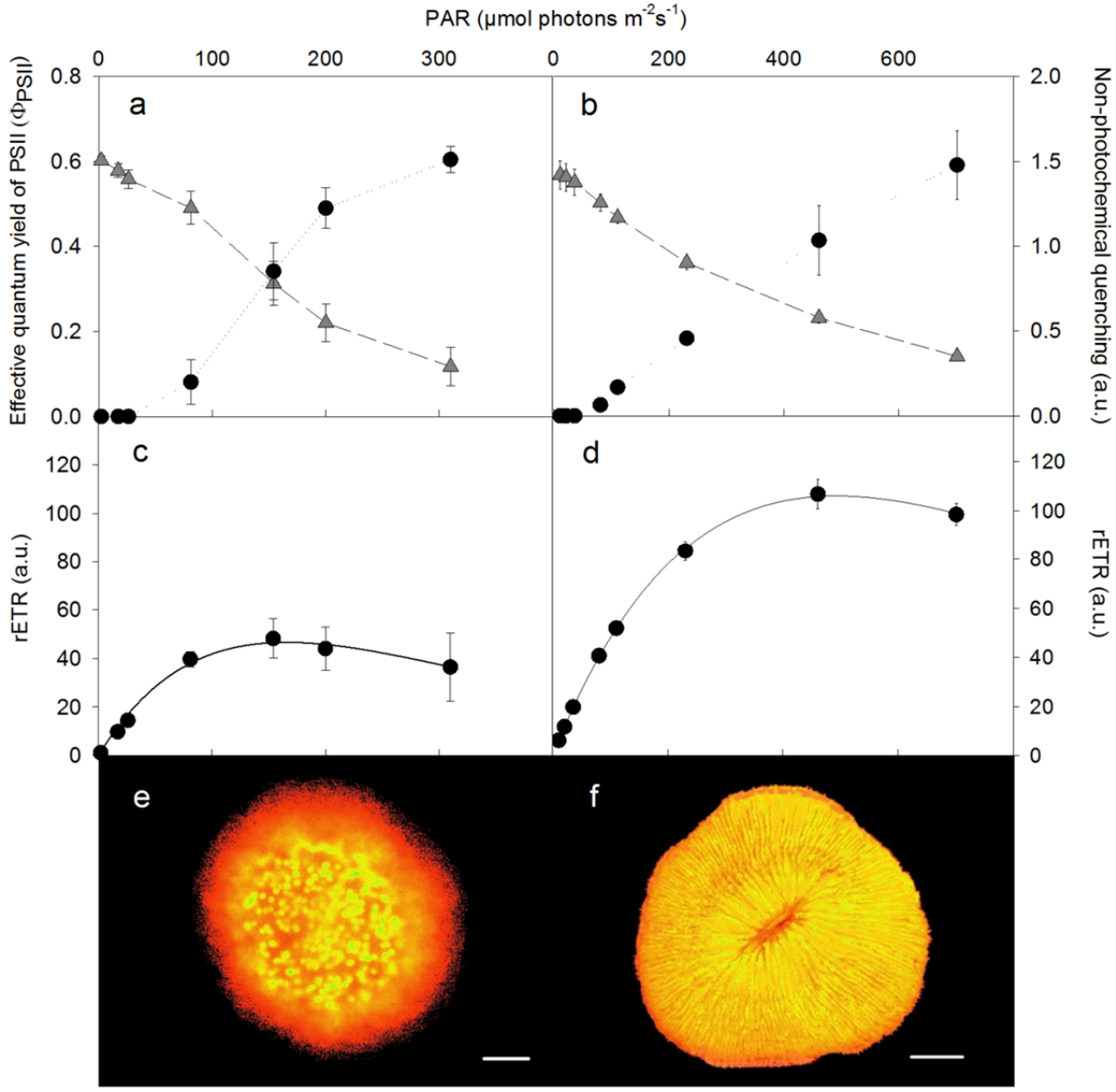

563

564

565 Figure 2

566

567

568

569

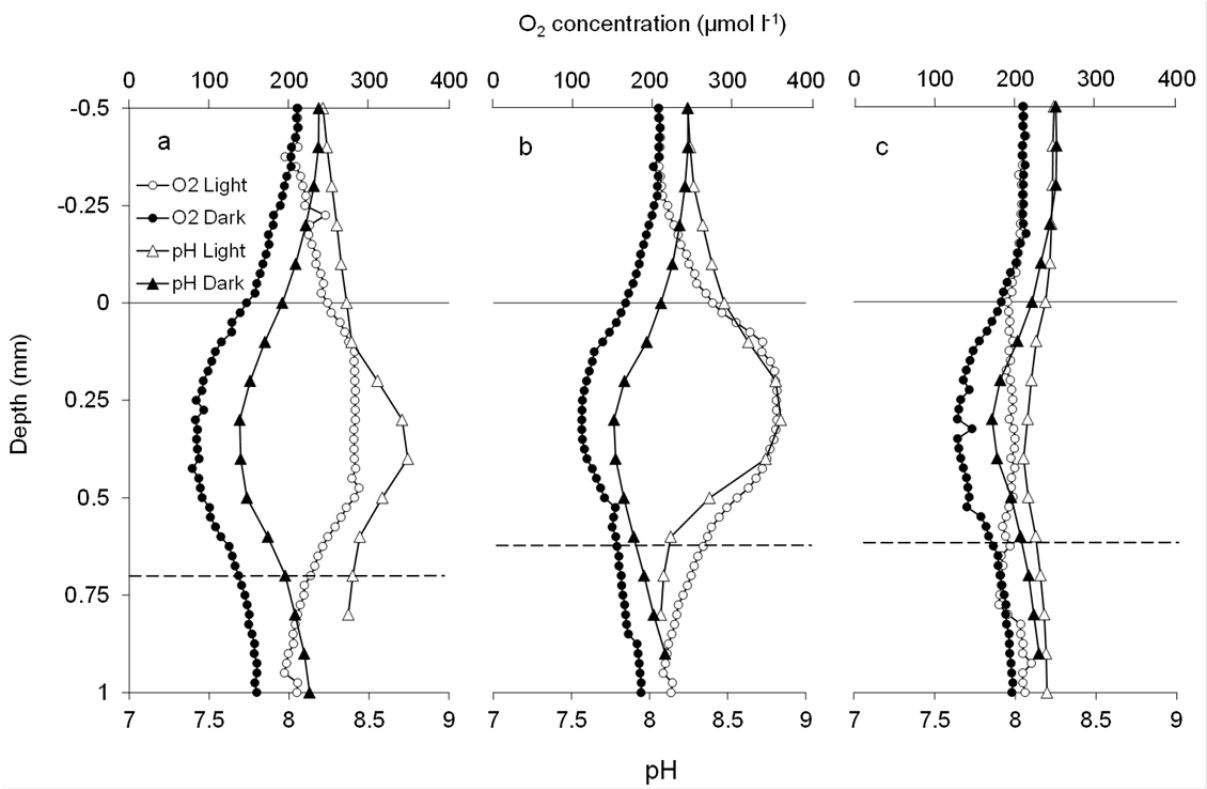
O2 concentration (µmol l-1)
0
100
200
300
400
a
b
c
O2 Light
O2 Dark
pH Light
pH Dark
Depth (mm)
-0.5
-0.25
0
0.25
0.5
0.75
1
7
7.5
8
8.5
9
pH

Figure 3

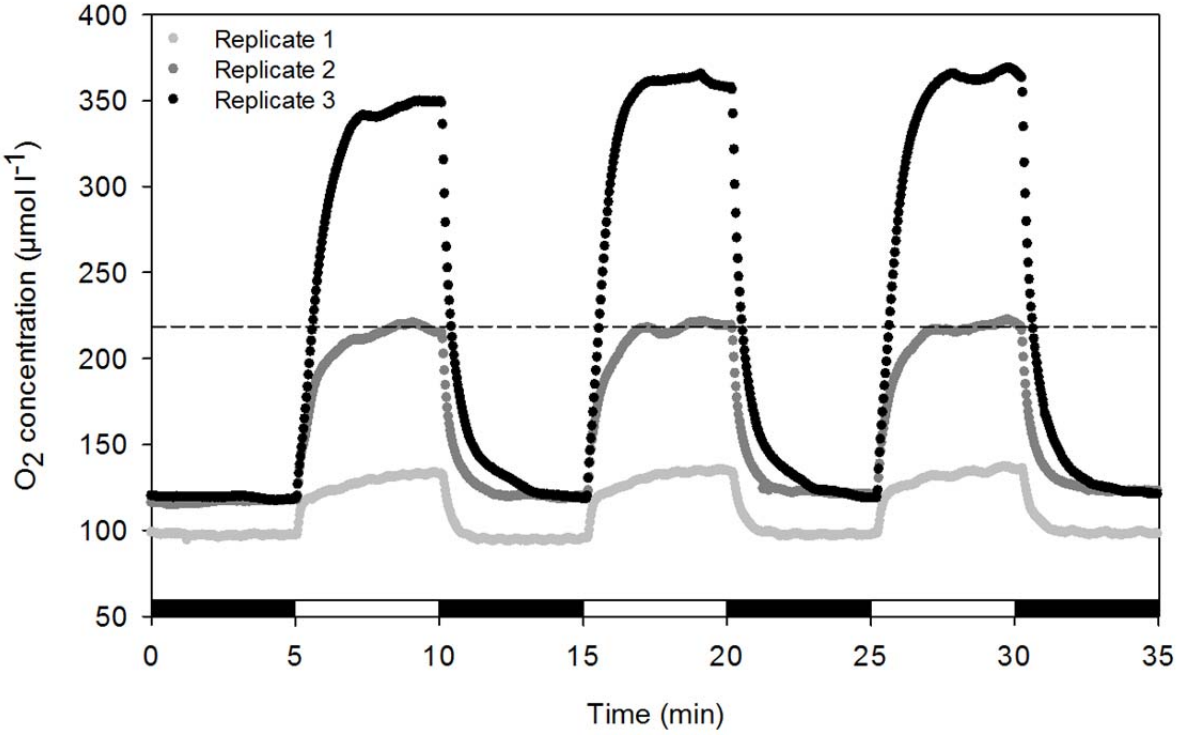

577

578

579

580 Figure 4

581